

## THERMAL EFFECT ON THE THERMOMECHANICAL BEHAVIOR OF CONTACTS IN A TRAVELING WAVE TUBE

by

**Mounir CHBIKI<sup>a,c</sup>, Tony DA SILVA BOTELHO<sup>b\*</sup>, Jean-Gabriel BAUZIN<sup>a</sup>,**  
**Najib LARAQI<sup>a\*</sup>, and Jean-Francois JARNO<sup>c</sup>**

<sup>a</sup> Paris Ouest University, Ville d'Avray, France

<sup>b</sup> Supmeca, Saint Ouen, France

<sup>c</sup> Thales Electron Devices, Vélizy-Villacoublay, France

Original scientific paper  
DOI: 10.2298/TSCI141216010C

*A new elasto-plastic study of the contact between the helix and the rods of the delay line of traveling waves tubes was realized. Our study is focused on the analysis of the hot lines shrinking phenomenon. In the studied case, unlike brazed configuration, the contact areas are not perfect, resulting in a diminution of the heat transfer process. In order to maximize the contact area and to homogenize the contact pressure, a soft thermal conductive material is coated on the helix; copper was chosen for this study. In the present work, an analytical model is used to identify the properties of the copper coating at a given temperature. Authors focused on the mechanical properties in order to improve the assembly process with a better numerical study. An experimental method has been made to validate the proposed model. The first comparison results seem to indicate that the model represents the reality with a good agreement. It is very clearly shown that the temperature decreases the mechanical properties (Young's modulus, yield strength, tensile strength, ...). And the thickness of the coating increases the contact area. This last point is less important at room temperature (6% of increase) than at 140 °C (22%).*

Key words: *thermal effect, traveling wave tubes, thermomechanical behavior, coating, plasticity*

### Introduction

Traveling wave tubes (TWT) are hyper frequency (up to 50 GHz) vacuum tubes used as power amplifier. The TWT consist of three parts (fig. 1), known as an electron gun (1), a transmission line (2), and a collector (3). The high frequency wave is injected at the electron gun side of the vacuum tube, containing a helix wire. This wave is then amplified by interaction with the electron beam. During this process, the helix materials experience a strong thermal dissipation that may cause damage. Therefore, it is required that such materials have a high thermal conductivity together with a quite strong electrical insulation. In addition, its geometry is quite complex due to the necessary interaction between the input wave and the electron beam for amplification.

In Chbiki *et al.* [1], an analytical modeling of thermal steady-state behavior of the TWT was proposed. In that work, each individual component thermal resistivity was first evaluated and then the global assembly thermal resistivity was determined as a function of individual resistivities and geometries. That global modeling allowed a parametric study of the TWT thermal resistivity.

\* Corresponding authors; e-mails: tony.dasilva@sumpeca.fr; nlaraqi@u-paris10.fr

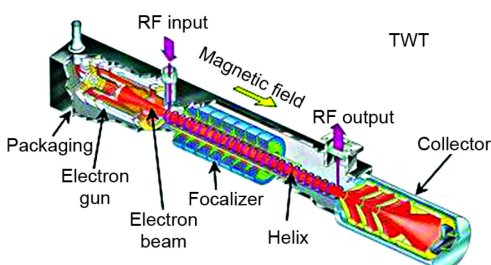


**Figure 1. Traveling-wave tube scheme**

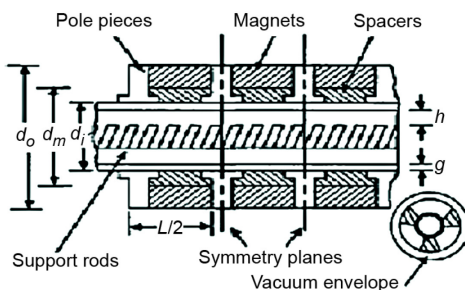


**Figure 2. Transmission line**

of that assembly. More specifically, the properties of the copper coating are of major interest.

Some performing techniques are available to access these mechanical properties, based on instrumented micro indentation tests [2-6] but the use of such instrumented devices make it difficult, if possible, to measure the coating properties with temperature, due to the limited access to samples and sensitivity of sensors. Some results are available on the temperature dependant properties of thin copper sheets of 12  $\mu\text{m}$  to 0.2 mm [7]. Another technique is then used to access these temperature dependant mechanical properties [2, 8]. This technique is also based on indentation, but instead of measuring the charge-discharge indentation curve, the analysis is focused on the measurement of the residual imprint. Since no sensor (else than temperature) is needed during the test, a wide range of temperatures is possible. An analytical model is then used to identify the properties of the copper coating at a given temperature.

### Modeling of the contact

The real helix/spacer contact is sphere/plan like, which justifies the use of a spherical indentation experimental technique, fig. 2.

To use the analytical model developed by Da Silva Botelho *et al.* [2], some assumptions are needed:

- the substrates are purely elastic, only the coating has an elasto-plastic behavior,
- the materials are homogeneous, isotropic,
- the coating has a linear hardening law (soft materials experience generally such a behavior),
- the depth penetration should be small compared with the thickness of the coating, and
- the interface coating/substrate should be perfectly adherent.

This model gives then an analytical relationship between the contact radius,  $a$  and the normal static load,  $W_N$ . The geometric description of the problem is given in fig. 3, where

Given the small dimensions of the TWT, the study of the thermo-mechanical behavior of interfaces is of major interest. Various processes were used to assemble TWT, leading to varied interface qualities. In the present work we focus on a specific contact between the helix and barrel, fig. 2. The thermal conductivity of that contact depends on the contact area and contact pressure, resulting from the assembling technique. In order to maximize the contact area and to homogenize the contact pressure, a soft, thermal conductive material is coated on the helix. In that application, copper was chosen. The shrinking technique used to assemble the helix together with the rods is known to provoke large plastic deformation of the copper coating, leading to an augmentation of the contact area, and a homogenization of the contact pressure.

Such a thermo-mechanical analysis can be performed numerically, using finite elements for example. But to achieve realistic results, one has to know adequate temperature-dependent mechanical properties of the constitutive materials

solids 1 and 2 are the indenter and the substrate, respectively, and solid 3 is the copper coating. Their respective Young's moduli and Poisson ratio are  $E_1$ ,  $E_2$ ,  $E_3$ ,  $\nu_1$ ,  $\nu_2$ , and  $\nu_3$ . The elastic limit of the coating is denoted  $Re_3$ . The elasto-plastic behavior of the copper is represented schematically in fig. 4. The plastic part of the curve is characterized by a tangent modulus,  $E_{II3}$ , related with Young's modulus as in eq. (1).

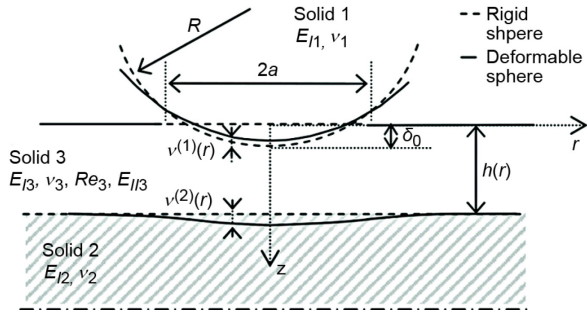


**Figure 3. Modeling of the soft coated contact problem [2]**

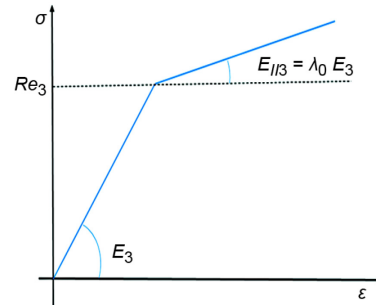


**Figure 4. Representation of the elasto-plastic behavior of the coating with linear hardening**

$$E_{II3} = \lambda E_3 \quad (1)$$

The model needs only two constants to describe the plastic part of the coating behavior:  $Re_3$  and  $E_{II3}$ .

The full resolution of the contact problem has been given by Da Silva Botelho *et al.* [2]. The main results of this work will now be summarized.

In case of elasto-plastic behavior of the coating, the relation between the normal load and the contact radius is given by eq. (2):

$$W_N = W_0 \frac{\bar{a}^4}{1+\bar{a}} \left[ 1 - (1-\lambda) \left( 1 - \frac{1+\bar{a}}{\bar{a}^2} Re_{eq} \right)^2 \right] \quad (2)$$

With the following constants and scaling values:

$$W_0 = \frac{\pi}{4} \left[ \frac{9\pi}{4(3\pi-4)} \right]^4 \frac{E_{12}^4 h^3}{E_{eq}^3 R} \quad (3)$$

$$\overline{Re_{eq}} = \frac{2Rh}{a_0^2 E_{eq}} Re_{eq} \quad (4)$$

$$\bar{a} = \frac{a}{a_0} = a \left[ \frac{9\pi}{4(3\pi-4)} \frac{E_{12}}{E_{eq}} h \right]^{-1} \quad (5)$$

$$E_{eq} = E_3 \left[ 1 - 2\nu_3 \frac{\frac{\nu_3 - \nu_2}{E_3} - \frac{\nu_2}{E_2}}{\frac{1 - \nu_3}{E_3} - \frac{1 - \nu_2}{E_2}} \right]^{-1} \quad (6)$$

$$Re_{eq} = Re_3 \left[ 1 + \frac{v_3}{1+v_3} \left( 1 - \frac{2}{v_3} \frac{\frac{v_2}{E_2} - \frac{v_3}{E_3}}{\frac{1-v_2}{E_2} - \frac{1-v_3}{E_3}} \right) \right]^{-1} \quad (7)$$

$$\lambda = \frac{E_{H2}}{E_3} \left( 1 - 2v_3 \frac{\frac{v_3}{E_3} - \frac{v_2}{E_2}}{\frac{1-v_3}{E_3} - \frac{1-v_2}{E_2}} \right) \left( 1 - 2v_3 \frac{\frac{v_3}{E_{H3}} - \frac{v_2}{E_2}}{\frac{1-v_3}{E_{H3}} - \frac{1-v_2}{E_2}} \right)^{-1} \quad (8)$$

In these equations,  $Re_{eq}$  represents the equivalent yield stress on the contact, including the behaviors of the substrates and the soft coating, and  $\lambda$  includes the boundary conditions of adhesion at the interface coating/substrate. The contact radius given by these equations is then used to evaluate the thermal contact resistance [10-12].

### Experimental and analytical results

To determine the mechanical constants of the copper elastoplastic behavior, a reverse engineering process is performed, using eqs. (2)-(8). An experimental campaign is then set-up on tungsten wires with copper coating but with a flat geometry instead of helix one to avoid the

structural contribution of the helix in the experimental results. The dimensions of the wire were 2 mm width and 0.4 mm thick. The coating was performed using a classical electrolysis technique. The wire width was 1 mm and the copper thicknesses were 3  $\mu\text{m}$  and 6  $\mu\text{m}$ .

A specific indenter (developed at Supmeca) was used to perform indentation tests on copper coated helix wires. The indenter kinematic diagram is presented in fig. 5. The normal load,  $W_N$ , is applied using weights and the dimensions of the contact area are measured after total unloading. Figure 6 gives an overview of the test bench and the geometry of the wire.

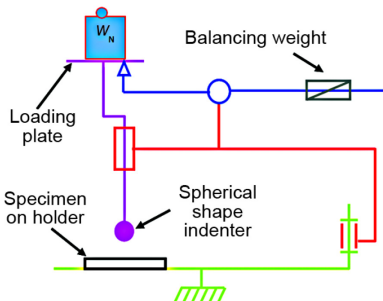


Figure 5. Indenter kinematic diagram

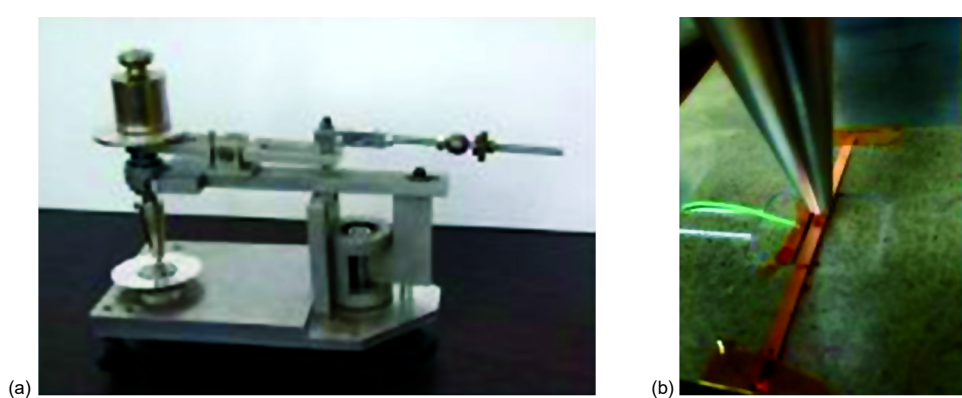


Figure 6. Global view of the indenter (a) and local view of the indentation process on a coated helix wire (b)

The indenter represents the rod material and was 1 mm diameter. Its initial microgeometry was controlled before the tests using a confocal surfometer. A balancing weight was used to compensate the own weight of the moving parts of the bench. A quasi-static loading is then performed, to avoid inertial effects. Seven successive loadings were performed at a given load to set up the dispersion of the results. Each imprint is the result of a unique test and a minimum distance between the imprints has been met (six times the indenter diameter). The contact was maintained for 15 seconds, a previous study showed that the time while kept in charge didn't affect the results [2].

The tested loads varied from 100 g to 3 kg. The lower boundary corresponds to the minimum load at which an imprint was detected and the upper boundary comes from the bench limitations.

Tests were performed at room temperature and at 140 °C. A portable heater was used to apply the temperature and a thermocouple was used to monitor the wire temperature during the test, fig. 7. For each tested temperature and each coating thickness, analysis of the contact radius vs. normal load curves were then exploited.

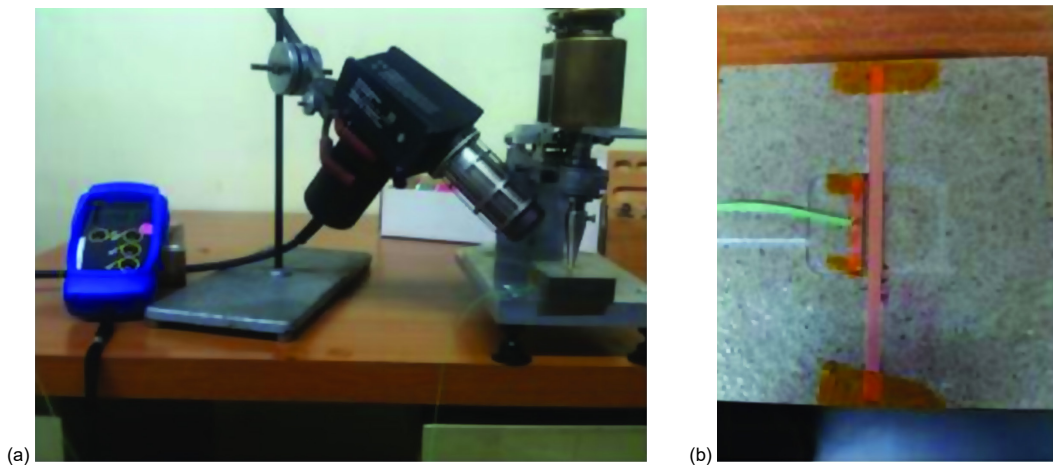
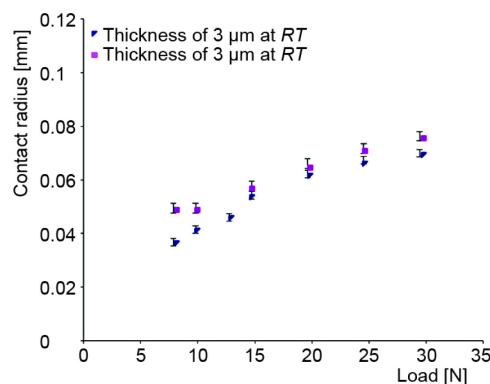


Figure 7. Portable heater (a) and thermocouple implantation (b) for temperature control

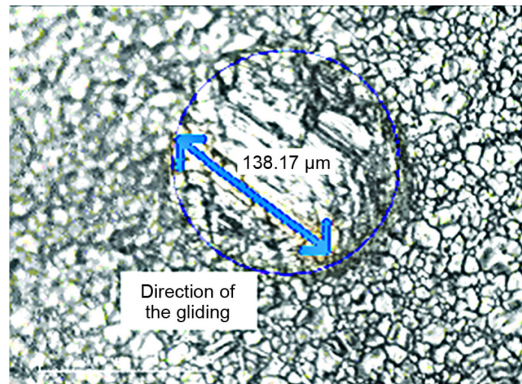
Figure 8 shows the influence of copper thickness on the evolution of contact radius with load. For the two tested thicknesses, the evolution of contact radius with load is quite similar. Despite the experimental dispersion, the two curves are clearly separated. For a given load, a thicker coating enables a larger contact radius. Unless for the two first points, the difference between the two curves is about 6%. The two first points, especially for 6 µm, differ from the global evolution. This experimental fact is related to the experimental apparatus: at low load, a transversal sliding component occurs, due to the apparatus kinematics, fig. 9.

Figure 10 exhibits the influence of temperature on the contact radius for a 3 µm thick coating. The higher the temperature, the larger the contact radius, which can be explained by the sensitivity of copper Young's modulus and yield strength with temperature [9]. Indeed, it is known that the mechanical properties decreases quickly above 100 °C, which explains that at a given load, the contact radius is larger when temperature is larger and that residual imprint can be measured at lower load when test temperature was higher. The two curves are well separated until about 17 N of normal load. After that value, both curves are similar, denoting a saturation

effect, related to the indenter radius and the penetration depth. That saturation can be considered as a limitation of the assumptions of the analytical model at 140 °C. At room temperature, such a saturation will occur at higher load, due to *stronger* mechanical properties.



**Figure 8. Influence of the coating thickness (triangles for 3.0  $\mu\text{m}$  and squares for 6.1  $\mu\text{m}$ ) at room temperature**



**Figure 9. Transversal sliding**

Figure 11 is similar to fig. 10, but with a 6  $\mu\text{m}$  thick coating. The very same conclusions can be drawn except for the saturation effect. In fact, the coating is thick enough to avoid the saturation at such loads. The saturation will most probably occur at higher load.

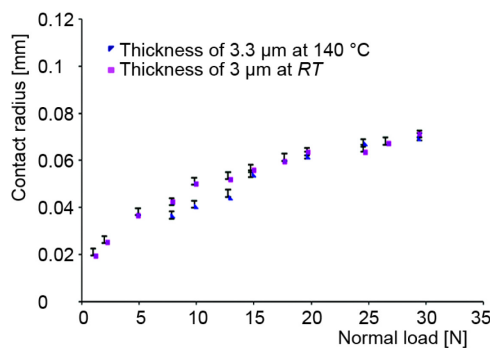


**Figure 10. Influence of temperature on the evolution of contact radius against normal load of a 3  $\mu\text{m}$  coating**

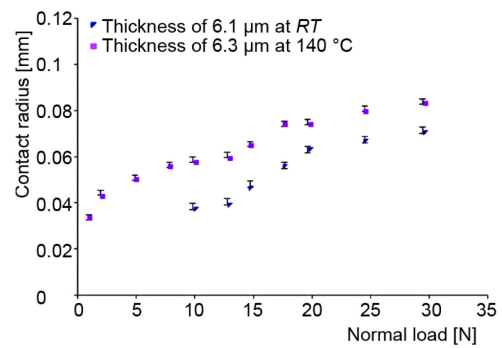


**Figure 11. Influence of temperature on the evolution of contact radius against normal load of a 6  $\mu\text{m}$  coating**

Figure 12 compares the evolution of contact radius for the two thicknesses at 140 °C. The two thicknesses have a similar evolution, but the difference between them is more pronounced at 140 °C than at room temperature. The difference between the two curves is about 22% (mean value). At room temperature, the difference was only about 6%. This evolution is to be compared to the evolution of mechanical properties of copper between room temperature and 140 °C.

From all these results, it is quite clear that to promote a larger contact radius, one has to select, among the operating conditions tested, the thickest coating and the highest temperature.

Once these experimental data established, next step is to compare them with the analytical model to identify mechanical constants.

Figures 13 and 14 present the experimental data at 3  $\mu\text{m}$  and 6  $\mu\text{m}$ , respectively, and the analytical model for various mechanical constants, expressed in terms of yield strength,  $Re$ , and tensile strength,  $Rm$ .

Analyzing the comparison between results for 3  $\mu\text{m}$  at 140 °C and analytical data, fig. 13, it seems that experimental data exhibits a transition from one analytical curve to the other, from the smoother one to the harder one. The very same conclusion can be drawn for 6  $\mu\text{m}$  at 140 °C, fig. 14. For the 6  $\mu\text{m}$  thick coating, the transition from copper properties to tungsten substrate properties is even clearer.

At room temperature, such a transition is not so clear, because of the lack of experimental data at low load. These comparisons brings out some information. One is to set the validity limit of our analytical model to normal loads less than 5 N for reverse engineering of experimental data. At higher load, the tungsten substrate becomes dominant on the copper coating, due to the not so small penetration depth compared to the coating thickness and indenter radius.

## Conclusions

This study allowed us to propose an analytical identification of the copper coating properties. It allows us to notice that the coating study can not be separated from the substrate study, even if it is much stiffer than the substrate.

The contact area increases with increasing thickness of the coating and that tendency is magnified by the effect of temperature. At room temperature, doubling the coating thickness increases the contact area by 6% for a given load whereas at 140 °C

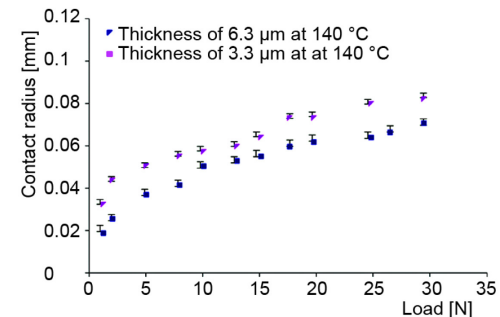


Figure 12. Influence of coating thickness at 140 °C

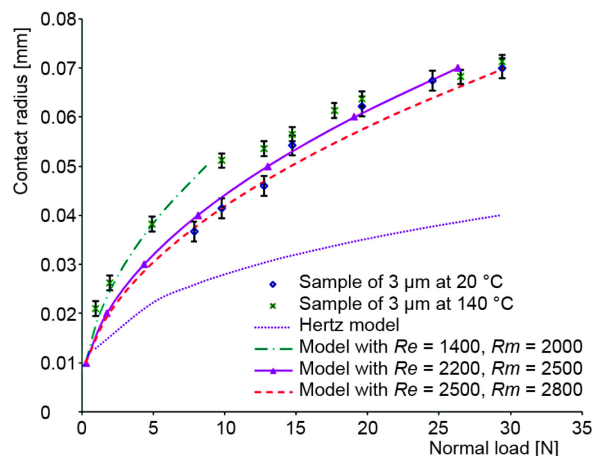


Figure 13. Comparison of experimental data and analytical model for the coating of 3  $\mu\text{m}$  thick

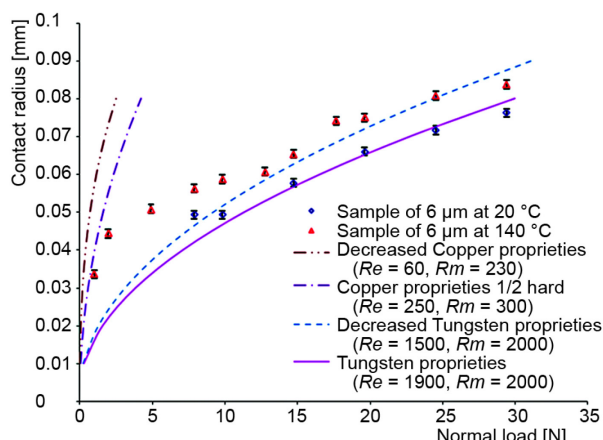


Figure 14. Comparison of experimental data and analytical model for the coating of 6  $\mu\text{m}$  thick

doubling the thickness results in an increase of the contact area by 22%. This effect is to be related to the evolution of mechanical properties of copper with temperature.

This study pointed out the influence of the temperature and the thickness of the coating on the evolution of the contact radius, which is a key feature for the thermal contact resistance. These results are to be used in a heat transfer study of a transmission line of traveling wave tubes.

### Acknowledgment

The authors wish to express their gratitude to Thales Electron Devices (TED) and l'Association Nationale de la Recherche et de la technologie (ANRT) for the technical and financial support granted to this study.

### Nomenclature

$a$	– contact radius, [mm]	$R$	– radius of solid 1 (spherical indenter), [mm]
$E_{12}$	– combined elastic modulus of materials 1 (indenter) and 2 (bulk material), [MPa]	$\bar{V}$	– normalized associated variable, for any variable $V$ ( $= v/v_0$ )
$E_{H3}$	– tangent modulus of the coating material (linear hardening model), [MPa]	$W_N$	– normal load, [N]
$E_i$	– Young's modulus of material $i$ , [MPa]	<i>Greek symbols</i>	
$h$	– thickness of the coating, [mm]	$\lambda$	– modulii ratio ( $= E_{H3}/E_3$ ), [-]
$R_{e3}$	– yield strength of the coating material (solid 3), [MPa]	$v_i$	– Poisson's ratio of material $i$ , [-]
$R_{eq}$	– apparent yield strength of the assembly, [MPa]		

### References

- [1] Chbiki, M., et al., Thermal Analysis of a Transmission Line of Traveling Wave Tube (TWT), *Proceedings, 6<sup>th</sup> European Thermal Sciences Conference*, Poitiers, France, 2012, Vol. 395
- [2] Da Silva Botelho, T., et al., Analytical and Experimental Elastoplastic Spherical Indentations of a Layered Half-Space, *Mech. Mater.*, 40 (2008), 10, pp. 771-779
- [3] Johnson, K. L., *Contact Mechanics*, Cambridge University Press, Cambridge, UK, 1985
- [4] Pharr, G., et al., Nanoindentation of Soft Films on Hard Substrates: Experiments and Finite Elements Simulations, *MRS Proceedings*, 505 (1997), 109
- [5] Vlassak, J., et al., Indentation Plastic Displacement Field: Part I, the Case of Soft Films on Hard Substrates, *J. Mater. Res.*, 14 (1999), 6, pp. 2196-2203
- [6] Tunvisut, K., et al., Use of Scaling Functions to Determine Mechanical Properties of Thin Coatings from Microindentation Tests, *Int. J. Solids Struct.*, 38 (2001), 2, pp. 335-351
- [7] Khatibi, G., et al., Temperature Dependent Elastic and Thermal Properties of Thin Copper Foils, in: *Copper: Better Properties for Innovative Products* (Ed. J.-M. Welter), Wiley-VCH Verlag Weinheim, Germany, 2007
- [8] Da Silva Botelho, T., et al., *Inverse Identification of Elastoplastic Characteristics Antifretting Coatings for Titanium Alloys* (in French), Journees Internationales Francophones de Tribologie (JIFT), Poitiers-Futuroscope, France, 2007
- [9] Arnaud, D., et al., Properties of Copper and Its Alloys (in French), in: *Techniques de l'Ingenieur* (M4640), 1985
- [10] Laraqi, N., Thermal Constriction Resistance of Coated Solids – Static and Sliding Contacts, *International Communications in Heat and Mass Transfer*, 26 (1999) 3, pp. 299-309
- [11] Laraqi, N., Bardon, J. P., Asperities Eccentricity Effect on the Thermal Constriction Resistance of Static or Sliding Contact, *Comptes rendus de l'Academie des Sciences – Serie IIb*, 326 (1998), 9, pp. 547-552
- [12] Laraqi, N., Bairi, A., Theory of Thermal Resistance between Solids with Randomly Sized and Located Contacts, *International Journal of Heat and Mass Transfer*, 45 (2002), 20, pp. 4175-4180

Paper submitted: December 16, 2014

Paper revised: January 3, 2015

Paper accepted: January 13, 2015

